Preprints of the 19th World Congress
The International Federation of Automatic Control
Cape Town, South Africa. August 24-29, 2014

Formation Control of Wheeled Robots in the Port-Hamiltonian Framework ⋆

Ewoud Vos [*,**] **Jacquelien M.A. Scherpen** [*]
Arjan J. van der Schaft [**] **Ate Postma** [*]

[*] *Research Institute of Technology and Management, University of Groningen, The Netherlands (e-mail: {e.vos,j.m.a.scherpen}@rug.nl, a.postma.14@student.rug.nl).*
[**] *Johann Bernoulli Institute for Mathematics and Computer Science, University of Groningen, The Netherlands (e-mail: a.j.van.der.schaft@rug.nl).*

Abstract: This paper proposes a new control strategy for the formation control of a network of wheeled robots. Starting from the rigid body dynamics, a dynamical model of the wheeled robot is derived in the port-Hamiltonian framework. The formation control objective is achieved by interconnecting the robots using virtual couplings, which give a clear physical interpretation of the proposed solution. Simulation and experimental results are given, to illustrate the effectiveness of the approach.

Keywords: Networked robotic system modeling and control, Mobile robots

1. INTRODUCTION

Mobile robots allow for completing a wide variety of tasks in unstructured environments. More recently there has been a growing interest in using groups of mobile robots to complete tasks, that can not be carried out by a single robot. For example Kurabayashi et al. [1996] propose an algorithm for sweeping a 2-dimensional area, while Obermeyer et al. [2011] study the deployment of multiple agents for coverage of polygonal environments.

The wheeled robot is a specific type of mobile robot that has been extensively studied in literature. The wheeled robot possesses a nonholonomic constraint on the motion of the robot. Many research has focused on the fact that due to this constraint, the wheeled robot does not meet Brockett's necessary condition on smooth feedback stabilization Brockett [1983]. This implies that the position and orientation of the robot can not be stabilized simultaneously using a time-invariant continuous controller. To overcome this problem, Lawton et al. [2003] and Bara and Dale [2009] stabilize only the position of the robot, neglecting the orientation.

Lawton et al. [2003] describe three types of formation control for multiple mobile robots: leader-following, behavioral, and virtual structures. Leader-following control assigns some robots as leaders, which should be followed by other robots (followers). For behavior-based control, several behaviors are described for each individual robot and the controller results from a weighting of these predescribed behaviors. In virtual structure control, the entire formation is considered as a (rigid) structure which should follow a trajectory as a whole. Both leader-following and virtual structures are easy to analyze, but require centralized controllers. Behavioral-based control on the other hand requires decentralized controllers, but as a result the collective behavior is much harder to analyze.

The contribution of this paper the derivation of a dynamical model of the wheeled robots in the port-Hamiltonian framework which is used to derive a distributed controller that guarantees formation control for a group of wheeled robots. The dynamics of the wheeled robot in the port-Hamiltonian framework are derived from the rigid body dynamics by eliminating the nonholonomic constraint to obtain the dynamics on the constrained state space. In alignment with Lawton et al. [2003] we control the position of the point $q_{C,i}$ on the robot, located at a distance $d_{AC,i} \neq 0$ from the axle (see Fig. 1). Controlling this point instead of the center of the axle $q_{A,i}$ is quite natural, since on-board sensors and/or end-effectors are usually not at the center of the axle. In addition to Lawton et al. [2003], we consider the dynamics of the robot rather than the kinematics. In addition to Bara and Dale [2009] we allow for both unicycle dynamics ($d_{AB,i} = 0$) as the more general wheeled robot dynamics, where the center of mass is not on the wheel axle ($d_{AB,i} \neq 0$). All these works focus on stabilizing the position rather than the orientation and are therefore not hindered by Brockett's necessary condition.

After deriving the robot's dynamics we introduce so-called virtual couplings, which we interconnect in between the wheeled robots. These virtual couplings give rise to a flexible virtual structure (since the couplings have dynamics), that controls the relative positions and relative velocities of the robots. The results are derived in the port-Hamiltonian framework, which is an energy-based modeling framework. Ortega et al. [2002] point out that the energy function in these type of models determines not only the static (stability), but also the transient behavior (performance). Moreover, energy concepts are well known and may therefore serve as a *lingua franca* amongst practitioners.

The outline of the paper is as follows. First the mathemat-

⋆ This work was supported in part by the Dutch Technology Foundation STW (ASSYS program, project 10550).

ical preliminaries and notation used are given. Then, in Section 2 the port-Hamiltonian dynamics of the wheeled robot are derived. Section 3 follows with the formation control using virtual couplings and the stability analysis. The simulation and experimental results are given in Section 4. The paper is wrapped up with a conclusion and outlook for future work.

Preliminaries The port-Hamiltonian framework is an energy-based framework which describes a large class of (nonlinear) systems including passive mechanical and electrical systems (see Duindam et al. [2009]). Control of these kind of systems is done via so-called power-ports, which consists of two port-variables (input $u \in \mathbb{R}^m$ and output $y \in \mathbb{R}^m$) who's product $u^T y$ equals the power supplied to the system. Let $x \in \mathbb{R}^n$ denote the state of the system, then the dynamics of a port-Hamiltonian system are given by

$$\begin{aligned} \dot{x} &= (J(x) - R(x)) \frac{\partial H}{\partial x}(x) + g(x)u \\ y &= g^T(x) \frac{\partial H}{\partial x}(x), \end{aligned} \tag{1}$$

with skew-symmetric structure matrix $J(x) \in \mathbb{R}^{n \times n}$ (i.e., $J(x) = -J^T(x)$), and positive semi-definite dissipation matrix $R(x) \in \mathbb{R}^{n \times n}$ (i.e., $R(x) = R^T(x) \geq 0$). The Hamiltonian $H(x)$ equals the total energy stored in the system, and its time derivative is given by $\dot{H} \leq u^T(t)y(t)$. Hence the increase in stored energy is always equal or smaller than the power supplied through the power-port (u, y). Therefore (1) is a passive system, if $H(x)$ is bounded from below (see Schaft [2000]). This property provides an excellent starting point for the stability analysis of many systems.

The interaction between the robots in the formation is described by an undirected connected graph $\mathcal{G}(\mathcal{V}, \mathcal{E})$, where $\mathcal{V}$ denotes the set of N vertices (robots) and $\mathcal{E} \subset \mathcal{V} \times \mathcal{V}$ denotes the set of M edges (virtual couplings). Robot i and j are interconnected by a virtual coupling if there is an edge $(i, j) \in \mathcal{E}$. Each edge has an orientation by assigning a positive sign to one end and a negative sign to the other end. The incidence matrix B associated to $\mathcal{G}(\mathcal{V}, \mathcal{E})$ describes which vertices are coupled by an edge, and is defined as

$$b_{ik} = \begin{cases} +1 & \text{if node } i \text{ is at the positive side of edge } k, \\ -1 & \text{if node } i \text{ is at the negative side of edge } k, \\ 0 & \text{otherwise.} \end{cases}$$

For more details on graphs see e.g. Bollobás [1998].

Notation Let $\ker A$ and $\mathrm{im} A$ denote respectively the kernel and image of matrix A. Let I_n denote the $n \times n$ identity matrix, and let all 0 elements be appropriately dimensioned matrices of all zeros. For a scalar function $H(x) \in \mathbb{R}$ and a vector $x \in \mathbb{R}^n$, let $\frac{\partial H}{\partial x}$ to denote the n-dimensional column vector of partial derivatives. Furthermore, for a vector function $S(x) \in \mathbb{R}^m$ let $\frac{\partial S}{\partial x}(x)$ the $m \times n$ Jacobian matrix. Finally, for $A \in \mathbb{R}^{m \times n}, B \in \mathbb{R}^{p \times q}$ let $A \otimes B$ denote the Kronecker product defined as

$$A \otimes B = \begin{pmatrix} a_{11}B & \cdots & a_{1n}B \\ \vdots & \ddots & \vdots \\ a_{m1}B & \cdots & a_{mn}B \end{pmatrix}.$$

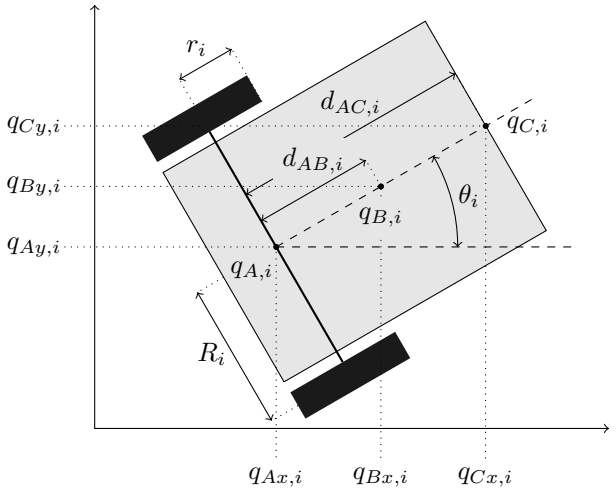

Fig. 1. Wheeled robot i

2. PORT-HAMILTONIAN MODEL OF THE WHEELED ROBOT

The setup of the wheeled robot i is depicted in Fig. 1. The point $q_{B,i}$ is the center of mass of the robot at a distance $d_{AB,i}$ from axle $q_{A,i}$. The point $q_{C,i}$ describes an arbitrary point in front of the robot at a distance $d_{AC,i} \neq 0$ from the axle, which is used for the controller design later on. Furthermore, let θ_i denote the orientation, r_i the radius of the wheels, and R_i the half axle length.

The dynamics of the wheeled robot are modeled as a rigid body with a nonholonomic constraint on its axle. Let $q_i \in \mathbb{R}^3$ denote the position, and let $p_i \in \mathbb{R}^3$ denote the corresponding momentum of robot i, where $q_i = (q_{Bx,i}, q_{By,i}, \theta_i)^T$ and $p_i = (p_{Bx,i}, p_{By,i}, h_i)^T$. The momentum is related to the position by $p_i = M_i \dot{q}_i$, with mass-inertia matrix $M_i = \mathrm{diag}\,(m_i, m_i, I_{cm,i})$ where m_i denotes the robot's mass and $I_{cm,i}$ denotes the moment of inertia around the center of mass $q_{B,i}$. The dynamics of the center of mass are now given by

$$\begin{aligned} \begin{pmatrix} \dot{q}_i \\ \dot{p}_i \end{pmatrix} &= \begin{pmatrix} 0 & I_3 \\ -I_3 & 0 \end{pmatrix} \begin{pmatrix} \dfrac{\partial H_i^r}{\partial q_i} \\ \dfrac{\partial H_i^r}{\partial p_i} \end{pmatrix} + \begin{pmatrix} 0 \\ G_i(q_i) \end{pmatrix} u_i \\ y_i &= G^T(q_i) \frac{\partial H_i^r}{\partial p_i}, \end{aligned} \tag{2}$$

where $u_i \in \mathbb{R}^2$, $y_i \in \mathbb{R}^2$, $H_i(p_i) \in \mathbb{R}$, $G_i(q_i)$, denote respectively, the input $u_i = (u_{f,i}, u_{\theta,i})^T$ (forward force, torque), the output $y_i = (y_{f,i}, y_{\theta,i})^T$ (forward velocity, angular velocity), the Hamiltonian $H_i^r(p_i) = \frac{1}{2} p_i^T M_i^{-1} p_i$, and the input matrix given by

$$G_i(q_i) = \begin{pmatrix} \cos\theta_i & 0 \\ \sin\theta_i & 0 \\ 0 & 1 \end{pmatrix}.$$

The nonholonomic constraint on the axle is given by

$$\sin\theta_i \dot{q}_{Ax,i} - \cos\theta_i \dot{q}_{Ay,i} = 0. \tag{3}$$

From Fig. 1 it is easily seen that $q_{Bx,i} = q_{Ax,i} + d_{AB,i} \cos\theta_i$ and $q_{By,i} = q_{Ay,i} + d_{AB,i} \sin\theta_i$. The corresponding velocities follow as $\dot{q}_{Bx,i} = \dot{q}_{Ax,i} - d_{AB,i} \sin\theta_i \dot{\theta}_i$ and $\dot{q}_{By,i} =$

$\dot{q}_{Ay,i} + d_{AB,i}\cos\theta_i\dot{\theta}_i$. Therefore (3) may be rewritten in terms of (2) as

$$\underbrace{\begin{pmatrix}\sin\theta_i & -\cos\theta_i & d_{AB,i}\end{pmatrix}}_{A_i^T(q_i)}\frac{\partial H_i^r}{\partial p_i}(p_i) = 0. \tag{4}$$

It is shown in Duindam et al. [2009] how we may solve for (4) to obtain the dynamics on the constrained state space. First note that $\text{rank}A_i^T(q_i) = 1$ and define the following matrix

$$S_i(q_i) = \begin{pmatrix}\cos\theta_i & -d_{AB,i}\sin\theta_i \\ \sin\theta_i & d_{AB,i}\cos\theta_i \\ 0 & 1\end{pmatrix}$$

such that $A_i^T(q_i)S_i(q_i) = 0$ and $\text{rank}S_i(q_i) = 2$. Now define $\bar{p}_i = \left(p_{f,i}, \bar{h}_i\right)^T$, $\bar{p}_{s,i}$ as

$$\begin{aligned}\bar{p}_i &:= S_i^T(q_i)p_i \\ \bar{p}_{s,i} &:= A_i^T(q_i)p_i\end{aligned} \qquad \bar{p}_i \in \mathbb{R}^2, \bar{p}_{s,i} \in \mathbb{R} \tag{5}$$

Clearly $(q_i, p_i) \mapsto (q_i, \bar{p}_i, \bar{p}_{s,i})$ defines a coordinate transformation, since the rows of $S_i(q_i)$ are orthogonal to the rows of $A_i(q_i)$. In the new coordinates, the $\bar{p}_s$ dynamics may be eliminated to obtain the following dynamics on the constrained state space

$$\begin{aligned}\begin{pmatrix}\dot{q}_i \\ \dot{\bar{p}}_i\end{pmatrix} &= \begin{pmatrix}0 & S_i(q_i) \\ -S_i^T(q_i) & \bar{C}_i(\bar{p}_i) - \bar{D}_i^r\end{pmatrix}\begin{pmatrix}\frac{\partial \bar{H}_i^r}{\partial q_i} \\ \frac{\partial \bar{H}_i^r}{\partial \bar{p}_i}\end{pmatrix} + \begin{pmatrix}0 \\ I_2\end{pmatrix}u_i \\ y_i &= \frac{\partial \bar{H}_i^r}{\partial \bar{p}_i},\end{aligned} \tag{6}$$

with Hamiltonian $\bar{H}_i^r = \frac{1}{2}\bar{p}_i^T\bar{M}_i^{-1}\bar{p}_i$, where $\bar{M}_i = \text{diag}\left(m_i, I_{cm,i}\right)$. The positive semi-definite matrix $\bar{D}_i^r \in \mathbb{R}^{2\times 2}$ is called the dissipation matrix, which is defined as $\bar{D}_i^r = \text{diag}\left(d_{f,i}, d_{\theta,i}\right)$. It models the forward and rotational friction of the robot.

The skew-symmetric matrix $\bar{C}_i(\bar{p}_i) \in \mathbb{R}^{2\times 2}$ captures the Coriolis and centrifugal forces, which are due to the center of mass not lying at the axis of rotation (the center of the axle) if $d_{AB,i} > 0$. The j,k-th element of $\bar{C}_i(\bar{p}_i)$ is defined by equation (2.142) in Duindam et al. [2009] as $\left(-(p_i)^T[S_j, S_k](q_i)\right)_{j,k}$, where $[S_j, S_k](q_i)$ denotes the Lie bracket of column j and k of matrix $S(q_i)$, in local coordinates q_i given as

$$[S_j, S_k](q_i) = \frac{\partial S_k}{\partial q_i}(q_i)S_j(q_i) - \frac{\partial S_j}{\partial q_i}(q_i)S_j(q_i).$$

Writing out the equations and using the fact that $\bar{h}_i = \frac{m_i d_{AB,i}^2 + I_{cm,i}}{I_{cm,i}}h_i$ (using (4),(5)) we obtain $\bar{C}_i(p_i)$ given by

$$\bar{C}_i(\bar{p}_i) = \begin{pmatrix}0 & \frac{m_i d_{AB,i}}{m_i d_{AB,i}^2 + I_{cm,i}}\bar{h}_i \\ -\frac{m_i d_{AB,i}}{m_i d_{AB,i}^2 + I_{cm,i}}\bar{h}_i & 0\end{pmatrix}.$$

Remark 1. The unicycle is a specific type of wheeled robot where the center of mass is on the axle of the robot. The unicycle dynamics can easily be obtained from (6) by setting $d_{AB,i} = 0$.

Remark 2. The well-known paper by Brockett [1983] provides a necessary condition under which systems can be stabilized using continuous feedback. From Proposition 4.2.14 by Schaft [2000] it follows that for (6) this condition boils down to

$$\bigcup_{\{x;\|x-x_0\|<\epsilon\}} (\text{im}J(q,\bar{p}) + \text{im}g(q)) = \mathbb{R}^6. \tag{7}$$

It is easily verified that (7) does not hold for (6) since

$$\text{im}\begin{pmatrix}0 & S_i(q_i) \\ -S_i^T(q_i) & \bar{C}_i(\bar{p}_i) - \bar{D}_i\end{pmatrix} + \text{im}\begin{pmatrix}0 \\ I_2\end{pmatrix} \subseteq \mathbb{R}^5.$$

However since we only control the position $q_{Cx,i}, q_{Cy,i}$ of the point $q_{C,i}$ and not the orientation θ_i our control objective is not hindered by (7).

For control purposes, we transform the input $u_i = (u_{f,i}, u_{\theta,i})^T$ into a new input $\bar{u}_i = (u_{x,i}, u_{y,i})^T$ where $u_{x,i}$ denotes a force along the x direction and $u_{y,i}$ denotes a force along the y direction. Both forces act on the point $q_{C,i}$ (see Fig. 1). The output y_i is transformed accordingly into the new output $\bar{y}_i = (y_{x,i}, y_{y,i})^T$. Bara and Dale [2009] provide the transformation $u_i \mapsto \bar{u}_i, y_i \mapsto \bar{y}_i$, which is given by

$$\begin{aligned}u_i &= \bar{G}_i(q_i)\bar{u}_i \\ \bar{y}_i &= \bar{G}_i^T(q_i)y_i,\end{aligned} \tag{8}$$

where

$$\bar{G}_i(q_i) = \begin{pmatrix}\cos\theta_i & \sin\theta_i \\ -d_{AC,i}\sin\theta_i & d_{AC,i}\cos\theta_i\end{pmatrix}.$$

Using (8) we can rewrite (6) as

$$\begin{aligned}\begin{pmatrix}\dot{q}_i \\ \dot{\bar{p}}_i\end{pmatrix} &= \begin{pmatrix}0 & S_i(q_i) \\ -S_i^T(q_i) & \bar{C}_i(\bar{p}_i) - \bar{D}_i^r\end{pmatrix}\begin{pmatrix}\frac{\partial H_i}{\partial q_i} \\ \frac{\partial H_i}{\partial \bar{p}_i}\end{pmatrix} + \begin{pmatrix}0 \\ \bar{G}_i(q_i)\end{pmatrix}\bar{u}_i \\ y_i &= \bar{G}_i^T(q_i)\frac{\partial H_i}{\partial \bar{p}_i},\end{aligned} \tag{9}$$

To compactly write the dynamics for all N robots denote the following state vectors $q_x = (q_{x,1}, \ldots, q_{x,N})^T$, $q_y = (q_{y,1}, \ldots, q_{y,N})^T$, $\theta = (\theta_1, \ldots, \theta_N)^T$, $q = (q_x, q_y, \theta)^T$, $\bar{p}_f = (\bar{p}_{f,1}, \ldots, \bar{p}_{f,N})^T$, $\bar{h} = \left(\bar{h}_1, \ldots, \bar{h}_N\right)^T$, $\bar{p} = \left(\bar{p}_f, \bar{h}\right)^T$. Furthermore define the following matrices

$$\begin{aligned}\sin\theta &= \text{diag}\left(\sin\theta_1, \ldots, \sin\theta_N\right), \\ \cos\theta &= \text{diag}\left(\cos\theta_1, \ldots, \cos\theta_N\right), \\ D_{AB} &= \text{diag}\left(d_{AB,1}, \ldots, d_{AB,N}\right), \\ D_{AC} &= \text{diag}\left(d_{AC,1}, \ldots, d_{AC,N}\right),\end{aligned}$$

$$\tilde{C}(\bar{p}) = \left(\frac{m_1 d_{AB,1}\bar{h}_1}{m_1 d_{AB,1}^2 + I_{cm,1}}, \ldots, \frac{m_N d_{AB,N}\bar{h}_N}{m_N d_{AB,N}^2 + I_{cm,N}}\right)^T,$$

$$\bar{C}(\bar{p}) = \begin{pmatrix}0 & \tilde{C}(\bar{p}) \\ -\tilde{C}(\bar{p}) & 0\end{pmatrix}, \quad S(q) = \begin{pmatrix}\cos\theta & -D_{AB}\sin\theta \\ \sin\theta & D_{AB}\cos\theta \\ 0 & I_N\end{pmatrix},$$

$$\bar{G}(q)\begin{pmatrix}\cos\theta & \sin\theta \\ -D_{AC}\sin\theta & D_{AC}\cos\theta\end{pmatrix}.$$

The dynamics (9) for all $i = 1, \ldots, N$ robots can now be compactly denoted by

$$\begin{pmatrix} \dot{q} \\ \dot{\bar{p}} \end{pmatrix} = \begin{pmatrix} 0 & S(q) \\ -S^T(q) & \bar{C}(\bar{p}) - \bar{D}^r \end{pmatrix} \begin{pmatrix} \dfrac{\partial H^r}{\partial q} \\ \dfrac{\partial H^r}{\partial \bar{p}} \end{pmatrix} + \begin{pmatrix} 0 \\ \bar{G}(q) \end{pmatrix} \bar{u}$$
$$y = \bar{G}^T(q) \frac{\partial H^r}{\partial \bar{p}}, \tag{10}$$

with Hamiltonian $\bar{H}^r = \frac{1}{2}\bar{p}^T \bar{M}^{-1} \bar{p}$, where

$$\bar{M} = \operatorname{diag}(m_1, \ldots, m_N, I_{cm,1}, \ldots, I_{cm,N}).$$

3. FORMATION CONTROL USING VIRTUAL COUPLINGS

To achieve formation control we interconnect the N wheeled robots using virtual couplings (i.e., virtual springs and dampers). This idea builds upon the theory of port-Hamiltonian systems on graphs (see Schaft and Maschke [2013]) and has been applied before to fully actuated systems in Vos et al. [2012] and satellites in Vos et al. [2013]. The main idea behind this approach is that we use a graph to describe the interconnection: the vertices of the graph correspond to the robots, the edges of the graph correspond to the virtual couplings.

Let $z_j \in \mathbb{R}^2$ denote the length along the x and y direction of the virtual coupling. The input to the control system $v_j \in \mathbb{R}^2$ is a velocity, while the corresponding output $w_j \in \mathbb{R}^2$ is a force. Furthermore let $D_j^v \in \mathbb{R}^{2\times 2}$ denote the corresponding damping matrix, defined as $D_j^v = \operatorname{diag}\left(d_{x,j}^v, d_{y,j}^v\right)$. The dynamics of virtual coupling j are given by

$$\begin{aligned} \dot{z}_j &= v_j \\ w_j &= \frac{\partial H_j^v}{\partial z_j}(z_j) + D_j^v v_j, \end{aligned} \tag{11}$$

with Hamiltonian $H_j^c(z_j) = \frac{1}{2}\left(z_j - z_j^*\right)^T K_j \left(z_j - z_j^*\right)$, where $z_j^* = \left(z_{x,j}^*, z_{y,j}^*\right)^T$ denotes the nominal spring length, and $K_j = \operatorname{diag}(k_{x,j}, k_{y,j})$ denotes the spring constants. Hamiltonian $H_j^c(z_j)$ corresponds to the energy stored in the virtual springs. Defining the springs in this way corresponds to position-based control in terms of Arcak [2007], which implies that not only the inter-robot distance, but also the inter-robot orientation is controlled.

Let $z_x = (z_{x,1}, \ldots, z_{x,M})^T$, $z_y = (z_{y,1}, \ldots, z_{y,M})^T$, $z = (z_x, z_y)^T$, $z_x^* = \left(z_{x,1}^*, \ldots, z_{x,M}^*\right)^T$, $z_y^* = \left(z_{y,1}^*, \ldots, z_{y,M}^*\right)^T$, $z^* = \left(z_x^*, z_y^*\right)^T$, denote the state and desired relative distance vector. Furthermore, define the following matrices

$$K_x = \operatorname{diag}(k_{x,1}, \ldots, k_{x,M}), K_y = \operatorname{diag}(k_{y,1}, \ldots, k_{y,M}),$$
$$D_x^v = \operatorname{diag}\left(d_{x,1}^v, \ldots, d_{x,M}^v\right), D_y^v = \operatorname{diag}\left(d_{y,1}^v, \ldots, d_{y,M}^v\right),$$
$$K = \operatorname{diag}(K_x, K_y), D^v = \operatorname{diag}\left(D_x^v, D_y^v\right).$$

Then we can compactly write the dynamics of (11) for $j = 1, \ldots, M$ as

$$\begin{aligned} \dot{z} &= v \\ w &= \frac{\partial H^v}{\partial z}(z) + D^v v, \end{aligned} \tag{12}$$

The incidence matrix B of the graph describes which robots (vertices) are interconnected by a virtual coupling (edges). For our purpose we choose a chain graph (or path graph) to describe this interconnection. The corresponding interconnection constraint (see Schaft and Maschke [2013], Vos et al. [2012], Vos et al. [2013]) is given by

$$\begin{cases} \bar{u} = -(I_2 \otimes B)\, w \\ v = (I_2 \otimes B)^T \bar{y} \end{cases} \tag{13}$$

The closed-loop network dynamics are obtained by eliminating (13) using (10),(12). Let $x = (q, \bar{p}, z)^T$, such that the closed-loop dynamics are given by

$$\dot{x} = (J(x) - R)\frac{\partial H}{\partial x}(x) \tag{14}$$

with closed-loop Hamiltonian $H(x) = H^r(\bar{p}) + H^c(z)$, and

$$J(x) = \begin{pmatrix} 0 & S(q) & 0 \\ -S^T(q) & \bar{C}(\bar{p}) & -\bar{G}(q)(I_2 \otimes B) \\ 0 & (I_2 \otimes B)^T \bar{G}^T(q) & 0 \end{pmatrix},$$
$$R = \begin{pmatrix} 0 & 0 & 0 \\ 0 & D^r + BD^vB^T & 0 \\ 0 & 0 & 0 \end{pmatrix}.$$

The control goal of static formation control can now be reformulated in terms of (14) as follows:

$$\begin{cases} z \to z^* \text{ for } t \to \infty \\ \bar{p} \to 0 \text{ for } t \to \infty \end{cases} \tag{15}$$

We are now ready to state the main result of this paper

Theorem 3. Consider N homogeneous wheeled robots (10) and M homogeneous virtual couplings (12). Interconnecting the wheeled robots (10) using virtual couplings (12) via interconnection constraint (13) achieves the control objective (15).

Proof. Take the closed-loop Hamiltonian $H(x)$ as a candidate Lyapunov function. Since $H(x)$ is quadratic in $\bar{p}$ and z, it follows that $H(x) \geq 0$ for all $x \in \mathbb{R}^{2N+2M}$. The time derivative $\dot{H}(x)$ follows from (14) and is given by

$$\dot{H}(x) = \frac{\partial^T H}{\partial x}(x)\dot{x} = -\frac{\partial^T H}{\partial x}(x) R \frac{\partial H}{\partial x}(x) \leq 0.$$

Now define the set $\mathcal{S} = \left\{ x \in \mathbb{R}^{2N+2M} \,\middle\|\, H(x) = 0 \right\}$. To find $\mathcal{S}$ note that for $D^r + BD^cB^T > 0$ we have that $H(x) = 0 \Rightarrow \bar{p} = 0$. Furthermore $\bar{p} = 0 \Rightarrow \dot{\bar{p}} = 0$, substituting into (14) gives

$$\begin{aligned} -\cos\theta B \frac{\partial H}{\partial z_x} - \sin\theta B \frac{\partial H}{\partial z_y}(z_y) = 0 \\ D_{AC}\sin\theta B \frac{\partial H}{\partial z_x} - D_{AC}\cos\theta B \frac{\partial H}{\partial z_y}(z_y) = 0 \end{aligned} \tag{16}$$

Multiplying the first line of (16) by $D_{AC}\cos\theta$, multiplying the second line by $\sin\theta$, and summing the result we obtain

$$D_{AC} B K_x (z_x - z_x^*) = 0. \tag{17}$$

Moreover, multiplying the first line of (16) by $D_{AC}\sin\theta$, multiplying the second line by $\cos\theta$, and summing the result we obtain

$$D_{AC} B K_y (z_y - z_y^*) = 0. \tag{18}$$

Since all diagonal elements of D_{AC}, K_x, K_y are equal (homogeneous robots and couplings) we obtain from (18)-(17) that $(z_x - z_x^*), (z_y - z_y^*) \in \ker B$. Since B represents the incidence matrix of a connected chain graph it follows that $z_x = z_x^*, z_y = z_y^*$ thereby completing the proof. ■

Parameter	Value
Mass $m_i[kg]$	0.167
Inertia $I_{cm,i}[kg \cdot m^2]$	$9.69 \cdot 10^{-5}$
Damping $d_{f,i}[kg/s]$	2
Damping $d_{\theta,i}[kg \cdot m^2/s]$	0.01
Distance $d_{AB,i}[m]$	$2 \cdot 10^{-3}$
Distance $d_{AC,i}[m]$	$20 \cdot 10^{-3}$
Wheel radius $r_i[m]$	$20.5 \cdot 10^{-3}$
Half axle length $R_i[m]$	$26.5 \cdot 10^{-3}$
Nominal spring length $z^*_{x,j}[m]$	0.3
Nominal spring length $z^*_{y,j}[m]$	$0.3(-1^{j+1})$
Spring constant $k_{x,j}, k_{y,j}[kg/s^2]$	1
Damping constant $d^v_{x,j}, d^v_{y,j}[kg/s]$	0

Table 1. Model parameters for the e-puck robot for $i = 1, \ldots, 5$, $j = 1, \ldots, 4$

Remark 4. The control law u for the robots is easily obtained from (8) and (13) and is given by $u = \bar{G}(q)\bar{u}$, with

$$\bar{u} = -\underbrace{(I_2 \otimes B)\frac{\partial H}{\partial z}(z)}_{\text{spring force}} - \underbrace{(I_2 \otimes B)D^v(I_2 \otimes B)^T\frac{\partial H}{\partial p}(p)}_{\text{damping force}} \tag{19}$$

Note that the presence of the incidence matrix B shows that (19) is in fact a distributed controller. Furthermore it is readily seen that only relative measurements are needed for implementation.

Remark 5. In this work we consider the *acyclic* path graph graph. This mean that Property 2.1 from Bai et al. [2011] (p.24) is satisfied for our setup, implying that there is a unique equilibrium point that corresponds to the desired formation. For *cyclic* graphs Property 2.1 might not be satisfied and undesired equilibria might pop up.

4. SIMULATION AND EXPERIMENTAL RESULTS

We illustrate the effectiveness of Theorem 3 by numerical simulations in MATLAB and experiments using the e-puck wheeled robot (see Fig. 2). The e-puck was developed by Mondada et al. [2009] for engineering education at the university level. Moreveover, due to the simple interface, it also provides an easy-to-use setup for experimental validation.

The experimental setup consists of $2.6 \times 2.0m$ table with a white plain white surface for localization of the robots. Each robot is identified and localized using a data-matrix, attached on top of each e-puck. A vision algorithm runs in parallel to MATLAB and provides the position and orientation of each e-puck using an overhead camera. MATLAB calculates the relative vectors between the e-pucks and the corresponding control input is then calculated using (19). This control input is than transformed into a common (linear velocity) and differential (angular velocity) input, which is send to the e-puck robot via Bluetooth. For the simulation we determined the model parameters for each e-puck robot modeled by (9) (see Table 1).

In both the simulations and the experiments we consider a network of $N = 5$ e-pucks interconnected by $M = 4$ virtual springs. The controller parameters are given in Table 1. Note that setting $D^v = 0$ has no effect on the converge result of Theorem 3, since $D^r > 0$. Virtual dampers allows us to tune the transient behavior of the e-pucks. However, at this moment the velocity measurements in the experimental setup are inaccurate and improvement is needed for proper implementation of the virtual dampers. The desired relative distances z^* are chosen according to a *zig-zag* formation, where the inter robot distance along respectively the x and y direction was set at $z^*_x = 0.3m$ and $z^*_y = \pm 0.3m$ accordingly. For a fair comparison, the initial conditions for the simulation were chosen in accordance with the initial conditions of the experiments. Both the simulation and the experiments were run for $t = 100s$.

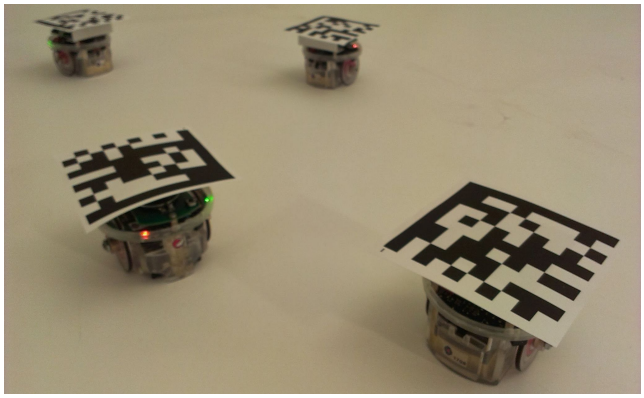

Fig. 2. Wheeled e-puck robot used in the experiments. The data-array on top is used for localization of the robot during the experiments

The trajectories for the robots are shown in Fig. 3. The (minor) differences between the simulation and the experiment can be explained by errors in the localization algorithm, saturation on the e-pucks inputs, and errors in the model parameter estimation. Both for the simulations (Fig. 3 top) and the experiments (Fig. 3 bottom) the robots converge to the desired zigzag formation. To clarify, we provide the time evolution of the relative distance z_x along the x direction (Fig. 4) and the time evolution of the relative distance z_y along the y direction (Fig. 5). As expected z_x converges to the desired distance z^*_x (Fig. 4), while z_y converges to z^*_y (Fig. 5).

5. CONCLUSION

In this paper we proposed a control law for the formation control of wheeled robots. The use of virtual couplings gives us a clear physical interpretation of the control law, which may serve as a *lingua franca* for engineers. The effectiveness of the algorithm was illustrated using simulations and experiments with the e-puck wheeled robot.

An extension using virtual walls in a similar fashion as discussed by Vos et al. [2012] is currently under investigation. The virtual walls provide a way to position the formation of robots on the plane. Another topic of interest is controlled movement of the formation, by making the virtual walls track a reference velocity.

REFERENCES

M. Arcak. Passivity as a design tool for group coordination. *IEEE Transactions on Automatic Control*, 52(8): 1380–1390, 2007. ISSN 0018-9286.

H. Bai, M. Arcak, and J. Wen. *Cooperative Control Design: A Systematic, Passivity-Based Approach*, volume 89. Springer, 2011.

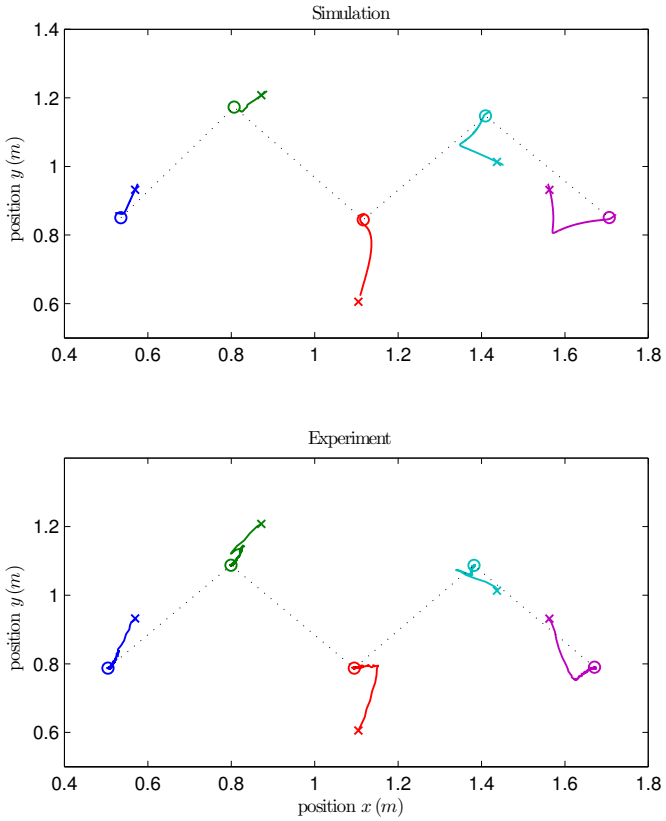

Fig. 3. Development of the formation from the inital position ($\times$) to the final position ($\circ$).

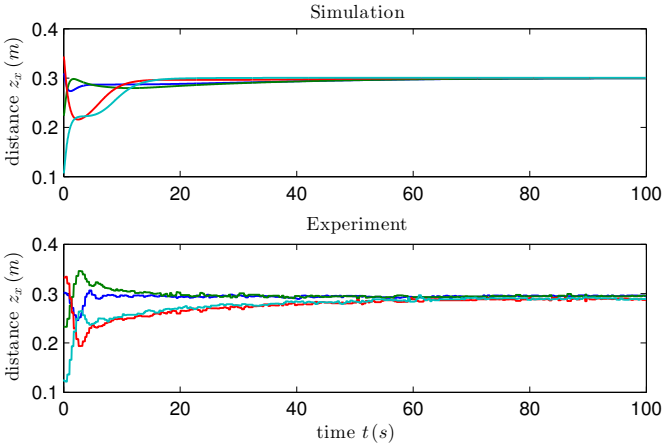

Fig. 4. Time evolution of the relative distance z_x along the x direction.

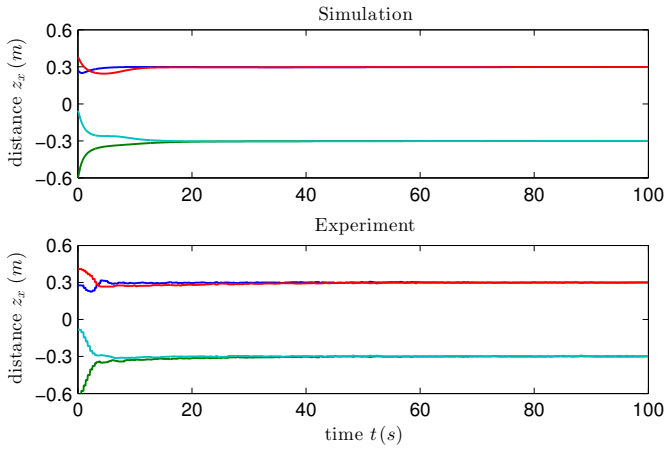

Fig. 5. Time evolution of the relative distance z_y along the y direction.

A. Bara and S. Dale. Dynamic modeling and stabilization of wheeled mobile robot. In *WSEAS International Conference on Dynamical Systems and Control*, number 11. WSEAS, 2009.

B. Bollobás. *Modern graph theory*, volume 184. Springer Verlag, 1998.

R.W. Brockett. *Asymptotic stability and feedback stabilization*. Birkhäuser, Boston, 1983.

V. Duindam, A. Macchelli, and S. Stramigioli. *Modeling and Control of Complex Physical Systems: The Port-Hamiltonian Approach*. Springer Verlag, 2009. ISBN 3642031951.

D. Kurabayashi, J. Ota, T. Arai, and E. Yoshida. Cooperative sweeping by multiple mobile robots. In *Robotics and Automation, 1996. Proceedings., 1996 IEEE International Conference on*, volume 2, pages 1744–1749. IEEE, 1996.

J.R.T. Lawton, R.W. Beard, and B.J. Young. A decentralized approach to formation maneuvers. *Robotics and Automation, IEEE Transactions on*, 19(6):933–941, 2003.

F. Mondada, M. Bonani, X. Raemy, J. Pugh, C. Cianci, A. Klaptocz, S. Magnenat, J.C. Zufferey, D. Floreano, and A. Martinoli. The e-puck, a robot designed for education in engineering. In *Proceedings of the 9th conference on autonomous robot systems and competitions*, volume 1, pages 59–65, 2009.

K. J. Obermeyer, A. Ganguli, and F. Bullo. Multi-agent deployment for visibility coverage in polygonal environments with holes. *International Journal of Robust and Nonlinear Control*, 21(12):1467–1492, 2011. ISSN 1099-1239.

R. Ortega, A. J. van der Schaft, I. Mareels, and B. Maschke. Putting energy back in control. *IEEE Control Systems Magazine*, 21(2):18–33, 2002. ISSN 0272-1708.

A.J. van der Schaft. *$\mathcal{L}_2$-gain and passivity techniques in nonlinear control*. Springer Verlag, 2000.

A.J. van der Schaft and B.M. Maschke. Port-Hamiltonian systems on graphs. *SIAM Journal on Control and Optimization*, 51(2):906–937, 2013.

E. Vos, J.M.A. Scherpen, and A.J. van der Schaft. Port-Hamiltonian Approach to Deployment. In *International Symposium on Mathematical Theory of Networks and Systems*, Melbourne, Australia, 9-13 July 2012.

E. Vos, J.M.A. Scherpen, and A.J. van der Schaft. Spatial Distribution of Satellite Constellations on Circular Orbits. In *IEEE Conference on Decision and Control*, Florence, Italy, 10-13 December 2013.